Article

Cell Reports

SEIPIN Regulates Lipid Droplet Expansion and Adipocyte Development by Modulating the Activity of Glycerol-3-phosphate Acyltransferase

Graphical Abstract

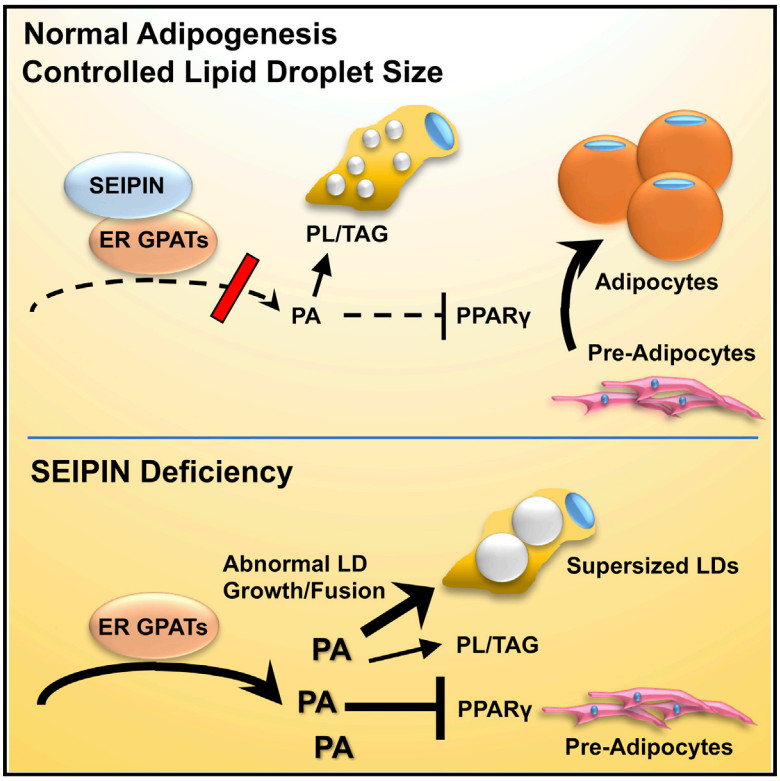

Authors

Martin Pagac, Daniel E. Cooper, Yanfei Qi, ..., Xun Huang, Rosalind A. Coleman, Hongyuan Yang

Correspondence

h.rob.yang@unsw.edu.au

In Brief

Pagac et al. find that SEIPIN, which has been linked to Berardinelli-Seip congenital lipodystrophy 2, interacts with microsomal glycerol-3-phosphate acyltransferase (GPAT) and influences its activity. Increased GPAT activity appears to underlie the block in adipogenesis and abnormal lipid droplet morphology associated with SEIPIN loss.

Highlights

- Loss of SEIPIN function causes Berardinelli-Seip congenital lipodystrophy 2
- Lack of SEIPIN increases glycerol-3-phosphate acyltransferase (GPAT) activity
- Inhibiting GPAT enhances differentiation of SEIPIN-deficient preadipocytes
- Inhibiting GPAT corrects abnormal lipid droplet morphology in SEIPIN deficiency

Pagac et al., 2016, Cell Reports *17*, 1546–1559
November 1, 2016
http://dx.doi.org/10.1016/j.celrep.2016.10.037

OPEN ACCESS
CellPress

Cell Reports
Article

SEIPIN Regulates Lipid Droplet Expansion and Adipocyte Development by Modulating the Activity of Glycerol-3-phosphate Acyltransferase

Martin Pagac,[1,8] Daniel E. Cooper,[2,8] Yanfei Qi,[1,8] Ivan E. Lukmantara,[1] Hoi Yin Mak,[1] Zengying Wu,[2] Yuan Tian,[3] Zhonghua Liu,[3] Mona Lei,[1] Ximing Du,[1] Charles Ferguson,[4] Damian Kotevski,[1] Pawel Sadowski,[1,9] Weiqin Chen,[5] Salome Boroda,[6] Thurl E. Harris,[6] George Liu,[7] Robert G. Parton,[4] Xun Huang,[3] Rosalind A. Coleman,[2] and Hongyuan Yang[1,10,*]

[1]School of Biotechnology and Biomolecular Sciences, University of New South Wales, Sydney, NSW 2052, Australia
[2]Department of Nutrition, University of North Carolina, Chapel Hill, NC 27599, USA
[3]State Key Laboratory of Molecular and Developmental Biology, Institute of Genetics and Developmental Biology, Chinese Academy of Sciences, Beijing 100101, China
[4]Institute for Molecular Bioscience, The University of Queensland, Queensland, QLD 4072, Australia
[5]Department of Physiology, Medical College of Georgia Regents University, Augusta, GA 30912, USA
[6]Department of Pharmacology, University of Virginia, Charlottesville, VA 22908, USA
[7]Institute of Cardiovascular Sciences and Key Laboratory of Molecular Cardiovascular Sciences, Ministry of Education, Peking University Health Science Center, Beijing 100191, China
[8]Co-first author
[9]Present address: Institute for Future Environments, Queensland University of Technology, Brisbane, QLD 4000, Australia
[10]Lead Contact
*Correspondence: h.rob.yang@unsw.edu.au
http://dx.doi.org/10.1016/j.celrep.2016.10.037

SUMMARY

Berardinelli-Seip congenital lipodystrophy 2 (BSCL2) is caused by loss-of-function mutations in SEIPIN, a protein implicated in both adipogenesis and lipid droplet expansion but whose molecular function remains obscure. Here, we identify physical and functional interactions between SEIPIN and microsomal isoforms of glycerol-3-phosphate acyltransferase (GPAT) in multiple organisms. Compared to controls, GPAT activity was elevated in SEIPIN-deficient cells and tissues and GPAT kinetic values were altered. Increased GPAT activity appears to underpin the block in adipogenesis and abnormal lipid droplet morphology associated with SEIPIN loss. Overexpression of *Gpat3* blocked adipogenesis, and *Gpat3* knockdown in SEIPIN-deficient preadipocytes partially restored differentiation. GPAT overexpression in yeast, preadipocytes, and fly salivary glands also formed supersized lipid droplets. Finally, pharmacological inhibition of GPAT in *Seipin*$^{-/-}$ mouse preadipocytes partially restored adipogenesis. These data identify SEIPIN as an evolutionarily conserved regulator of microsomal GPAT and suggest that GPAT inhibitors might be useful for the treatment of human BSCL2 patients.

INTRODUCTION

Congenital generalized lipodystrophy (CGL; also known as Berardinelli-Seip congenital lipodystrophy [BSCL]) is an autosomal recessive disorder characterized by a near total loss of adipose tissue, severe hypertriglyceridemia, insulin resistance, and fatty liver (Agarwal and Garg, 2006; Magré et al., 2001). To date, four genes have been linked to CGL/BSCL: 1-acylglycerol-3-phosphate-O-acyltransferase-2 (*AGPAT2*)/CGL1, *SEIPIN*/CGL2, *CAVEOLIN-1*/CGL3, and *CAVIN-1*/CGL4 (Fei et al., 2011a). The most severe form of human CGL/BSCL is caused by loss-of-function mutations in *SEIPIN*/*BSCL2*, which encodes an integral membrane protein of the endoplasmic reticulum (ER) with no recognizable functional domains (Fei et al., 2011a; Cartwright and Goodman, 2012; Lundin et al., 2006). *Seipin* knockout (*Bscl2*$^{-/-}$) mice have severe lipodystrophy and insulin resistance (Cui et al., 2011; Chen et al., 2012; Prieur et al., 2013), demonstrating an essential role for *Seipin* in adipogenesis. SEIPIN and its non-mammalian orthologs also control the expansion of lipid droplets (LDs). The most prominent feature of *Seipin*-deficient cells is the formation of "supersized" LDs (Fei et al., 2008, 2011b; Szymanski et al., 2007; Tian et al., 2011; Jiang et al., 2014; Liu et al., 2014). Thus, SEIPIN has a unique role in regulating both systemic (adipogenesis) and cellular (LD expansion) lipid storage.

Recent studies implicate SEIPIN and its yeast ortholog, Fld1 (also known as Sei1), in regulating phospholipid metabolism such that the amount of phosphatidic acid (PA) is increased in SEIPIN-deficient cells and tissues (Fei et al., 2011c; Sim et al., 2012; Jiang et al., 2014; Wolinski et al., 2015; Han et al., 2015). We have postulated that in preadipocytes, increased PA acts as a peroxisome proliferator-activated receptor gamma (PPARγ) antagonist and thus blocks adipogenesis (Stapleton et al., 2011; Fei et al., 2011a). In non-preadipocytes and yeast, PA promotes LD expansion, likely because it is fusogenic (Fei et al., 2011c). However, exactly how the ER-localized SEIPIN might regulate the metabolism of phospholipids remains unknown.

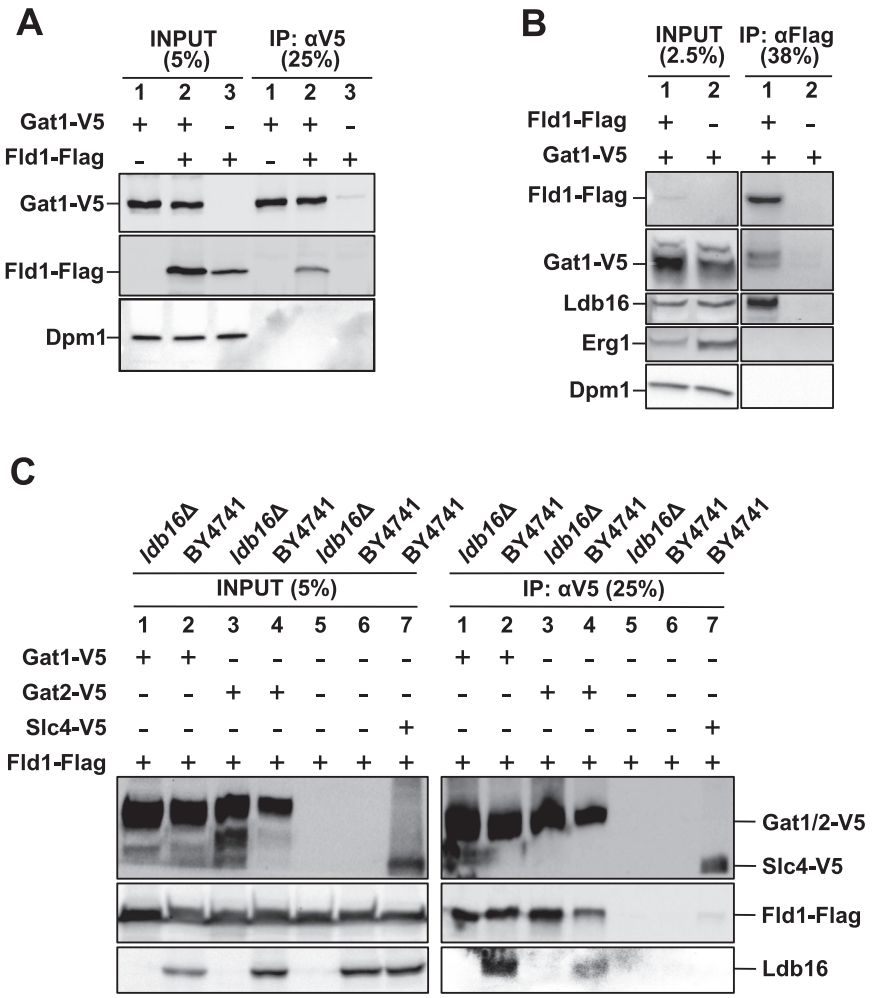

Figure 1. Fld1, Ldb16, and Gat1/2 Interact in Yeast

(A) Co-immunoprecipitation assay detecting the interaction between overexpressed Gat1-V5 and Fld1-FLAG in yeast lysates.

(B) Gat1-V5 and Ldb16 of endogenous level co-immunoprecipitate with Fld1-FLAG.

(C) Using V5 antibody, overexpressed Fld1-FLAG co-immunoprecipitates with overexpressed Gat1-V5 and Gat2-V5 from wild-type and *ldb16Δ* yeast lysates.

See also Figure S1 and Table S1.

Through affinity isolation and tandem mass spectrometry analyses, we identified proteins that specifically co-precipitate with Fld1-GFP in the yeast *Saccharomyces cerevisiae*. The most prominent of these proteins was Gat1, a glycerol-3-phosphate acyltransferase (GPAT). As the rate-limiting step in the synthesis of triacylglycerol and glycerophospholipids, GPAT catalyzes the esterification of glycerol-3-phosphate with a long-chain acyl-coenzyme A (acyl-CoA) to initiate the formation of PA (Cao et al., 2012; Marr et al., 2012; Wendel et al., 2009). We found that mammalian SEIPIN specifically interacted with the corresponding mammalian GPAT orthologs, GPAT3 and GPAT4. SEIPIN deficiency in yeast, mammalian cells, and mouse tissues resulted in increased GPAT activity and changes in GPAT kinetics. These data strongly suggest that SEIPIN is an evolutionarily conserved regulator of GPAT and that targeting GPAT may have therapeutic potential in treating BSCL2.

RESULTS

Fld1 and Gat1 Physically Interact

To identify potential Fld1/SEIPIN-interacting proteins, we used the native promoter of *FLD1* on a low-copy plasmid in wild-type or *fld1*Δ yeast cells to express GFP alone or a functional Fld1-GFP fusion protein (Fei et al., 2008). Cell membranes were isolated and solubilized using three different buffer conditions, followed by affinity purification and tandem mass spectrometry analyses (see Experimental Procedures).

In all three buffer/lysis conditions used, 19 proteins co-precipitated with Fld1-GFP, but not with matrix or GFP alone (Figure S1A; Table S1). Because our previous studies strongly suggested that Fld1/SEIPIN regulates cellular PA content (Fei et al., 2011c; Tian et al., 2011; Jiang et al., 2014), we focused on the yeast GPAT, Gat1, which catalyzes the rate-limiting step in the de novo synthesis PA and all glycerolipids. Tagged and overexpressed Fld1 and Gat1 were co-immunoprecipitated from yeast (Figure 1A), and this interaction was retained when both proteins were expressed at close to endogenous levels by adding tags at the C termini of their respective genomic loci (Figure 1B). As recently reported (Wang et al., 2014), we also identified Ldb16 as an Fld1-interacting protein in our screen (Figure S1A; Table S1), and endogenous Ldb16 co-immunoprecipitated with both Fld1-FLAG (Figure 1B) and Gat1 (Figure 1C). Furthermore, Fld1 and Ldb16 also co-immunoprecipitated with Gat2, a second yeast GPAT that shares ~38% sequence identity and ~58% sequence similarity with Gat1 (Figures 1C and S1B). However, a yeast AGPAT homolog, Slc4, did not co-immunoprecipitate with Fld1 as well as Gat1/2 (Figure 1C). Fld1-Gat1/2 interaction was not affected in *ldb16* null cells (Figure 1C), but we were not able to test whether the Ldb16 and Gat1/2 interaction requires Fld1, because Ldb16 is extremely unstable in the absence of Fld1 (Wang et al., 2014; data not shown).

Mammalian SEIPIN and GPAT3/4 Physically Interact

Mammals express four GPAT isoforms; GPAT1 and GPAT2 are present on the outer mitochondrial membrane, and GPAT3 and GPAT4 are present on the ER (Coleman and Mashek, 2011). GPAT1 is resistant to N-ethylmaleimide (NEM), whereas the other GPATs are sensitive to NEM. SEIPIN co-immunoprecipitated with

both GPAT3 and GPAT4 in 3T3L1 preadipocytes (Figure 2A). The interaction was significantly weakened (by ~50%) between GPAT3/4 and the SEIPIN missense mutant (T78A) that causes a human lipodystrophy (Sim et al., 2013) (Figures 2B and 2C, lane 3; Figures S1D and S1E). The C-terminal cytoplasmic region of SEIPIN was not essential for the interaction with GPAT3 or GPAT4, because SEIPIN C-terminal truncation mutants could still co-precipitate a significant amount of GPAT3/4 (Figure S1C). Importantly, overexpressed SEIPIN immunoprecipitated endogenous GPAT3/4 (the commercial antibody recognizes both GPAT3 and GPAT4) (Figure 2D). As an alternative approach, in mature adipocytes, we expressed SEIPIN that was fused to the promiscuous biotin ligase BirA* (Roux et al., 2012). After affinity purification with streptavidin-conjugated beads, GPAT3/4 was detected only in cells expressing SEIPIN-BirA*, but not SEIPIN or BirA* alone (Figure 2E). These data indicate that GPAT3/4 in adipocytes lies in close proximity to SEIPIN. Finally, we employed a proximity ligation assay to further examine the SEIPIN-GPAT3/4 interaction in vivo (Söderberg et al., 2006). GPAT3 and GPAT4 are closer to SEIPIN than AGPAT2 (Figure S2A) and, consistent with Figure S1C, full-length SEIPIN, but not its C terminus, interacted strongly with GPAT3/4 (Figures S2B and S2C). To examine the effects of SEIPIN on GPAT3/4 localization, 3T3-L1 preadipocytes were co-transfected with mCherry-SEIPIN or small hairpin RNA (shRNA) targeting SEIPIN and GFP-tagged mouse GPAT3 or GPAT4 and treated with fatty acids. GPAT3 primarily localizes to LDs, and SEIPIN overexpression or knockdown had little effect on GPAT3 localization (Figures S3A, S3B, and S3D). GPAT4 localizes to both ER and LDs, and SEIPIN knockdown increased the proportion of GPAT4 on LDs (Figures S3C, S3E, and S3F).

GPAT Activity Is Increased in SEIPIN-Deficient Cells and Tissues

To test whether SEIPIN interacts with GPAT to regulate its activity, we measured GPAT activity in control and SEIPIN-deficient yeast cells, mammalian cells, and mouse testes. In the absence of SEIPIN, the protein expression of the microsomal GPAT isoforms was virtually unchanged (Figures S4A–S4C). However, GPAT-specific activity in *fld1 null* yeast cells was ~60% higher than in controls (Figure 3A). In *Seipin*$^{-/-}$ mouse embryonic fibroblasts (MEFs), the total and microsomal GPAT activities were twice as high as in control MEFs (Figures 3B and S4C). Similarly, when *Seipin* was knocked down by ~70% in 3T3L1 preadipocytes, GPAT activity was twice as high as in control preadipocytes (Figures 3C, S4D, and S4E), and in mouse testes, where *Seipin* is normally highly expressed, total, NEM-sensitive (GPAT2, 3&4) and NEM-resistant (GPAT1) GPAT activities were 67%, 75%, and 29% higher, respectively, in *Bscl2*$^{-/-}$ testes than in controls (Figures 3D and S4F). Taken together, these data demonstrate that SEIPIN downregulates GPAT activity and that this regulatory role is conserved from yeast to mammals.

SEIPIN-Deficient Cells and Tissues Had Altered GPAT Kinetics

Next, we investigated GPAT enzyme kinetics by characterizing the affinity of GPAT for its substrates, glycerol-3-phosphate (glycerol-3-P) and long-chain acyl-CoA. Because acyl-CoAs are amphipathic and may act as detergents to disrupt membranes and inhibit enzyme activity (Polokoff and Bell, 1978), the apparent K_M values for acyl-CoAs often cannot be accurately calculated. In the absence of SEIPIN, the affinity of GPAT for glycerol-3-P or palmitoyl-coenzyme A (palmitoyl-CoA) was altered in MEFs, 3T3L1 cells (Figures 3E–3H and S4G–S4J), yeast, and *Bscl2*$^{-/-}$ mouse testis (Figures S4K–S4N). In each case, GPAT-specific activity and V_{max} increased (Table S2).

Increased GPAT Activity Underpins the Change in LD Morphology in SEIPIN-Deficient Cells

The above data indicate that SEIPIN interacts with GPAT to inhibit its activity. Although the immediate product of GPAT catalysis is lysophosphatidic acid, GPAT is the rate-limiting step, and the next enzyme in this synthetic pathway, lysophosphatidic acyltransferase, rapidly converts lysophosphatidic acid (LPA) to PA. Thus, increasing GPAT activity increases the level of PA in mammalian cells (Zhang et al., 2012a, 2014). In yeast, elevated PA in the ER is associated with the formation of "supersized" LDs in *fld1* null cells (Fei et al., 2011c), which had higher GPAT activity (Figures 3 and S4G–S4J). Is the increase in GPAT activity sufficient to raise the amount of PA on the ER and drive the formation of supersized LDs? Indeed, overexpressing wild-type, but not "catalytically dead," *GAT1* and *GAT2* in yeast cells caused supersized LDs to form (Figures 4A and S5A), phenocopying *fld1* null cells. The level of PA in the ER was higher in these cells, similar to *fld1* null cells, as indicated by increased *INO1* expression (Figure S5B) (Loewen et al., 2004). As detected by mass spectrometry, overexpression of GAT2 increased microsomal PA (Figure 4B). Importantly, when either *GAT1* or *GAT2* was co-expressed with *FLD1*, the amount of PA in the ER was reduced and few supersized LDs were detected (Figures 4A, 4B, and S5B). These results suggest that loss of Fld1 increases GPAT activity and the level of PA in the ER, causing the formation of supersized LDs.

Supersized LDs are also present in SEIPIN-deficient mature adipocytes and testes, tissues in which SEIPIN is normally highly expressed (Jiang et al., 2014; Liu et al., 2014). Overexpressing both GPAT3 and GPAT4 in 3T3-L1 preadipocytes increased microsomal PA and formed enlarged LDs (Figures 4C–4E and S5C), but as in yeast, overexpressing SEIPIN together with GPAT3 and GPAT4 reduced LD size and microsomal PA (Figures 4C–4E). Moreover, knocking down *Seipin*/*Bscl2* in 3T3 L1 preadipocytes increased the size of LDs, a feature that was reversed by knocking down either *Gpat3* or *Gpat4* (Figures S5D and S5E). In Huh7 cells, where there is little SEIPIN expression, overexpressing GPAT3 or GPAT4 alone can dramatically increase LD size (Figure S5F). To further investigate the functional relationship between SEIPIN and GPAT at system level, we examined the morphology of the larval salivary gland of *Drosophila*. Numerous globular structures are present in *dSeipin* mutants (Figure 5A) (Tian et al., 2011), and these structures can be encircled by a lipid droplet surface marker PLIN1-mCherry (Figure 5B), indicating that they are lipid droplets. *GPAT* (*Drosophila* gene *CG5508*) overexpression results in large lipid droplets similar to *dSeipin* mutants (Figure 5C), while overexpressing *AGPAT* (*CG17608*), *Lipin* (*CG8709*), or *DGAT* (*CG31991*) using

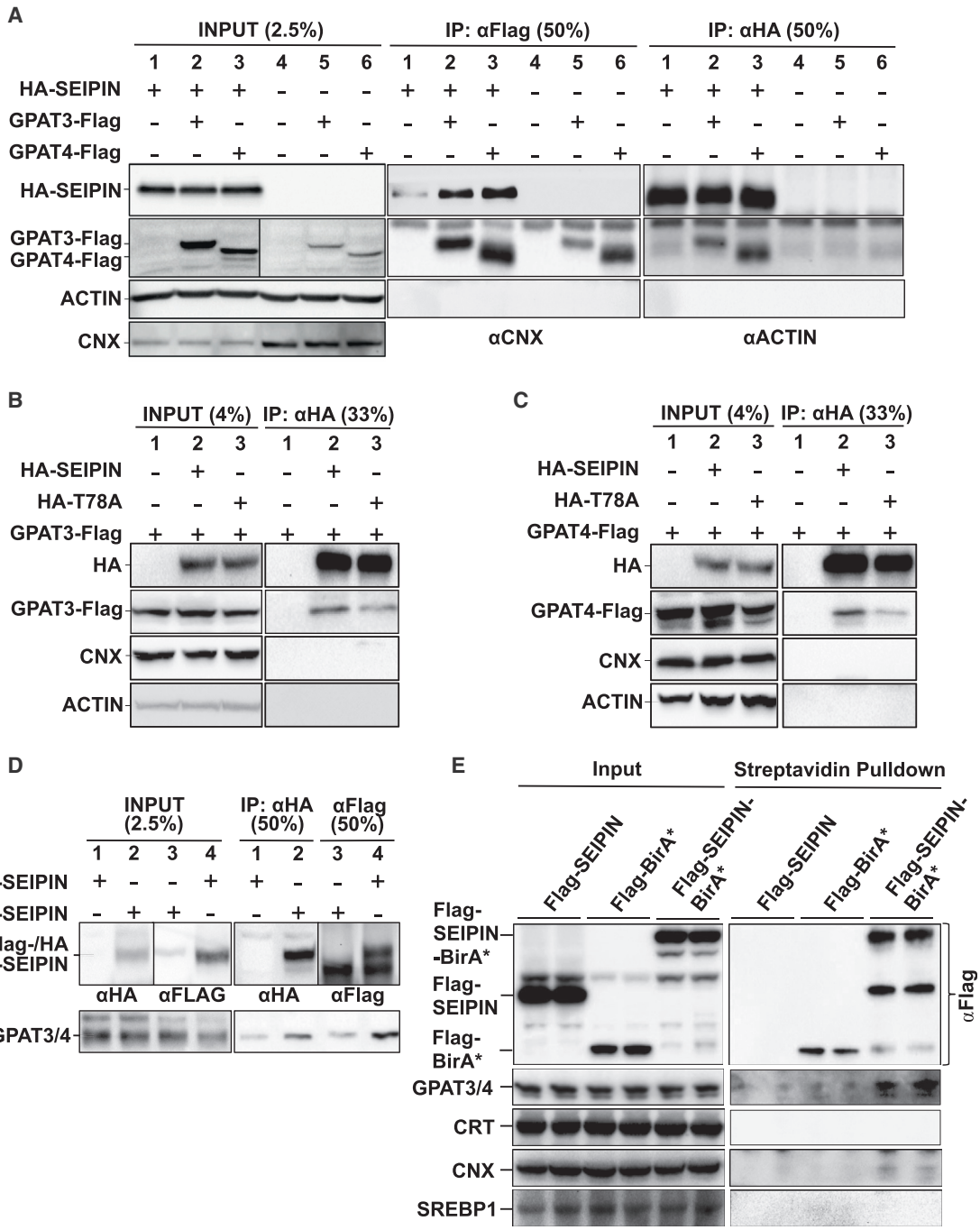

Figure 2. Mammalian SEIPIN and GPAT3/4 Physically Interact

(A) Co-immunoprecipitation by FLAG and hemagglutinin (HA) antibody of overexpressed FLAG-tagged GPAT3 or GPAT4 and HA-tagged SEIPIN, respectively, from transfected 3T3-L1 cell lysates.

(B and C) Immunoblotting for overexpressed HA-tagged mutant or wild-type SEIPIN and FLAG-tagged GPAT3 and GPAT4, respectively, after HA-immunoprecipitation from 3T3-L1 cells. See also Figure S2.

(D) Endogenous GPAT4 and GPAT3 proteins co-immunoprecipitate with overexpressed SEIPIN from 3T3-L1 adipocytes stably transfected with HA- or FLAG-SEIPIN.

(E) 3T3-L1 adipocytes expressing FLAG-SEIPIN, FLAG-tagged biotin ligase BirA*, or FLAG-tagged BirA*-SEIPIN were treated with 50 μM biotin for 24 hr. The biotinylated proteins were pulled down using streptavidin-conjugated agarose from biological duplicates. Elutes were subjected to western blot analysis. All experiments were performed in triplicate.

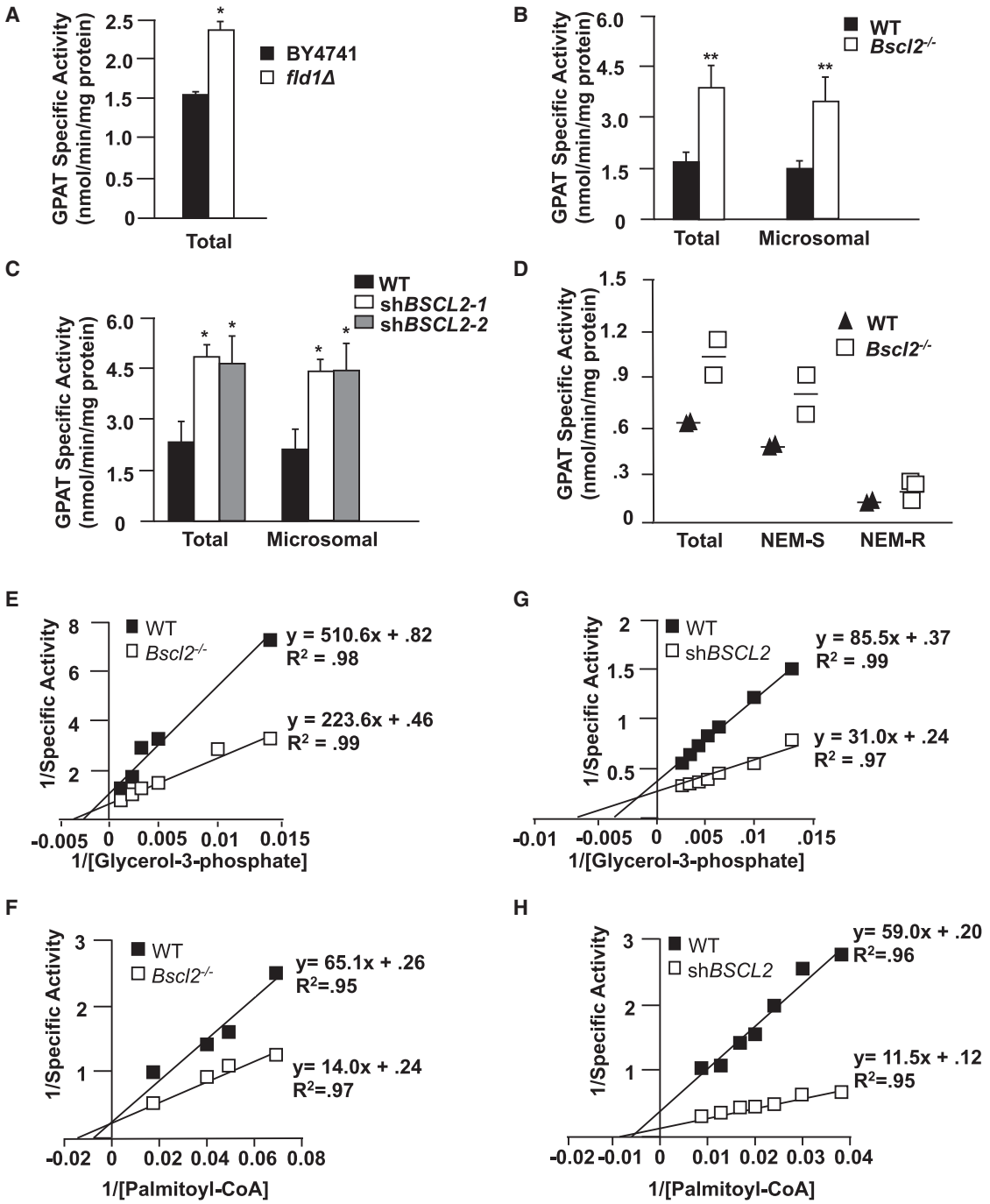

Figure 3. GPAT Activity Is Significantly Increased and GPAT Kinetics Are Altered in SEIPIN-Deficient Cells and Tissues

(A–D) GPAT specific activity (initial rates) was measured in total membrane preparations from (A) BY4741 and *fld1*Δ yeast, (B) control and *Bscl2*$^{-/-}$ mouse embryonic fibroblasts, (C) control and *shBSCL2* 3T3L1 preadipocytes, and (D) control and *Bscl2*$^{-/-}$ testes. Membrane proteins were incubated on ice for 15 min in the presence or absence of 2 mM NEM. Experiments were performed in triplicate. Data are presented as mean ± SEM. See also Figure S4.

(E–H) GPAT dependence on glycerol-3-phosphate or Palmitoyl-CoA in control and *Bscl2*$^{-/-}$ testis (E and F) and control and *shBSCL2* 3T3-L1 preadipocytes (G and H). Glycerol-3-phosphate and palmitoyl-CoA concentrations were varied as indicated. Double-reciprocal plots are shown in Figures S4G–S4J. All experiments were performed in triplicate. Data are presented as mean ± SEM.

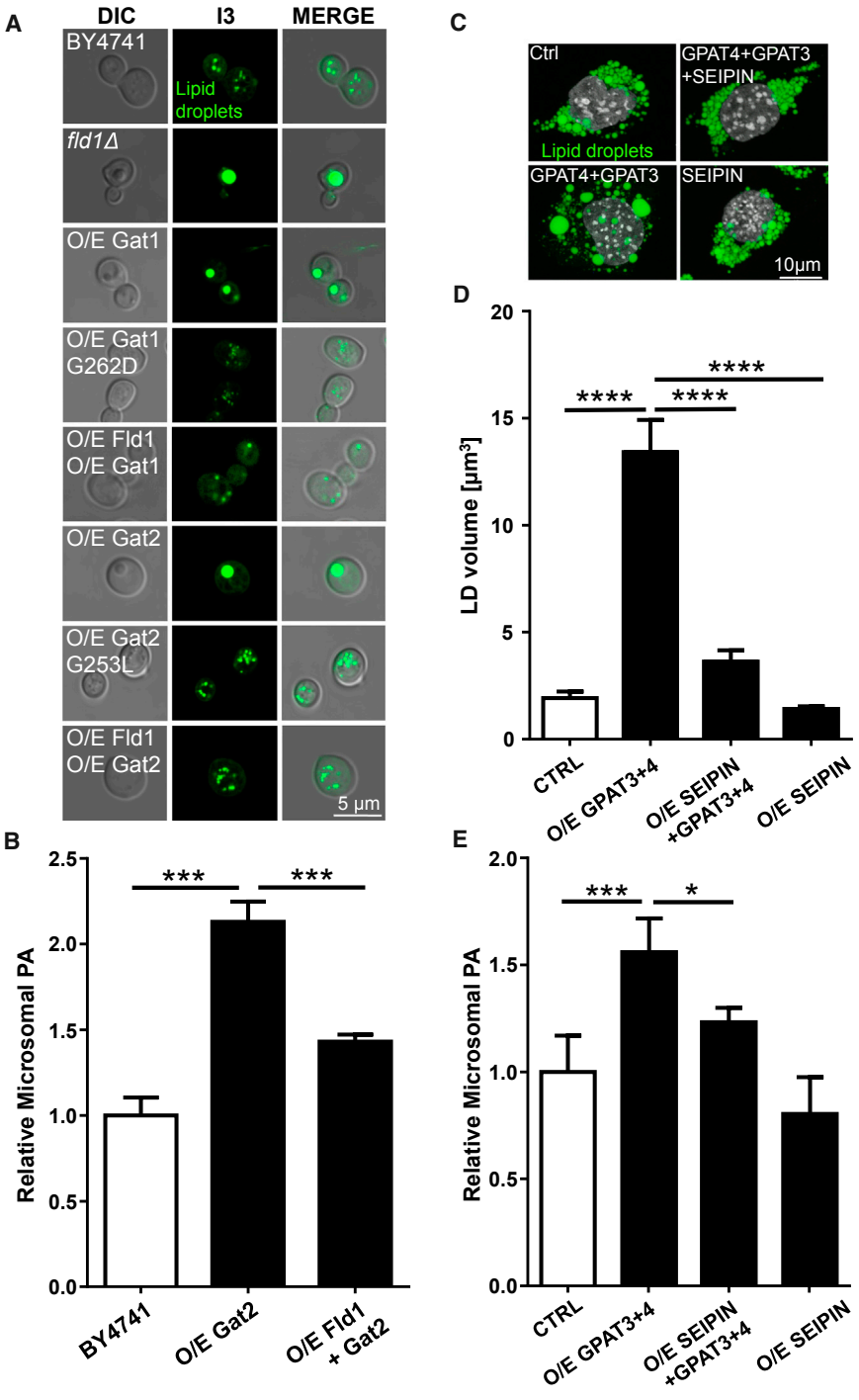

Figure 4. Increased GPAT Activity Underpins the Change in LD Morphology in SEIPIN-Deficient Cells

(A) Nile-red-stained lipid droplets of BY4741 wild-type (WT), *fld1*Δ, *GAT1*-, or *GAT2*-overexpressing strains (O/E Gat1 and O/E Gat2), strains overexpressing catalytically dead *gat* mutants (O/E Gat1 G262D and O/E Gat2 G253L), and double-transformed strains (O/E Gat1 + O/E Fld1 and O/E Gat2 + Fld1). The cells were grown to early stationary phase.

(B and E) Lipidomic analysis of microsomal PA in the indicated yeast strains and transduced preadipocytes. Phospholipids were extracted from cells, subjected to HPLC MS/MS, and analyzed using Lipid Search software. n = 4. *$p < 0.05$; **$p < 0.01$; ***$p < 0.001$.

(C) BODIPY-stained lipid droplets in 3T3-L1 preadipocytes, transduced with indicated lentiviral expression vectors and incubated with 400 μM oleate for 16 hr. Representative confocal images are shown.

(D) Diameters of top three largest lipid droplets in 100 of each cell line were measured to determine the droplet volumes. Data represent mean ± SD (****$p < 0.0001$).

See also Figure S5.

the same promoter leads to many tiny lipid droplets. *ACAT* (*CG8112*) overexpression forms small lipid droplets and aberrant patch-like structures. Finally, knocking down *dSEIPIN* in *Drosophila* S2 cells increased LD size, which was suppressed by knocking down *GPAT* simultaneously (Figure 5D). Together, these results strongly suggest that increased GPAT activity underpins the formation of supersized LDs in SEIPIN-deficient cells and tissues.

During Early Differentiation, SEIPIN Alters GPAT Kinetics

In addition to its role in modulating LD expansion, SEIPIN is required for normal adipogenesis. Loss of *Seipin* disrupts adipogenesis within the first few hours of differentiation (Chen et al., 2012; Payne et al., 2008). We asked whether this feature was also related to SEIPIN's ability to regulate GPAT activity and PA metabolism. We first examined whether the level of PA is disturbed in *Seipin* knockdown 3T3-L1 preadipocytes by mass spectrometry. As shown in Figures 6A and 6B, total microsomal PA and the majority of PA species were significantly increased upon SEIPIN depletion. We then examined GPAT kinetics during the differentiation of 3T3L1 preadipocytes. In wild-type (WT) cells, the apparent K_M values for glycerol-3-P after 0, 4, 8 and 12 hr of differentiation were 176, 267, 176, and 153 μM, respectively (Figure S6A), consistent with a transient drop in affinity for glycerol-3-P at 4 hr. In contrast, the apparent K_M values for glycerol-3-P in *Seipin* knockdown cells at the same time points were 113, 147, 142, and 138 μM, respectively, values considerably lower than in the control cells (Figures S6B and S6C). These findings suggest the possibility that SEIPIN regulates GPAT kinetics early during differentiation to regulate PA homeostasis.

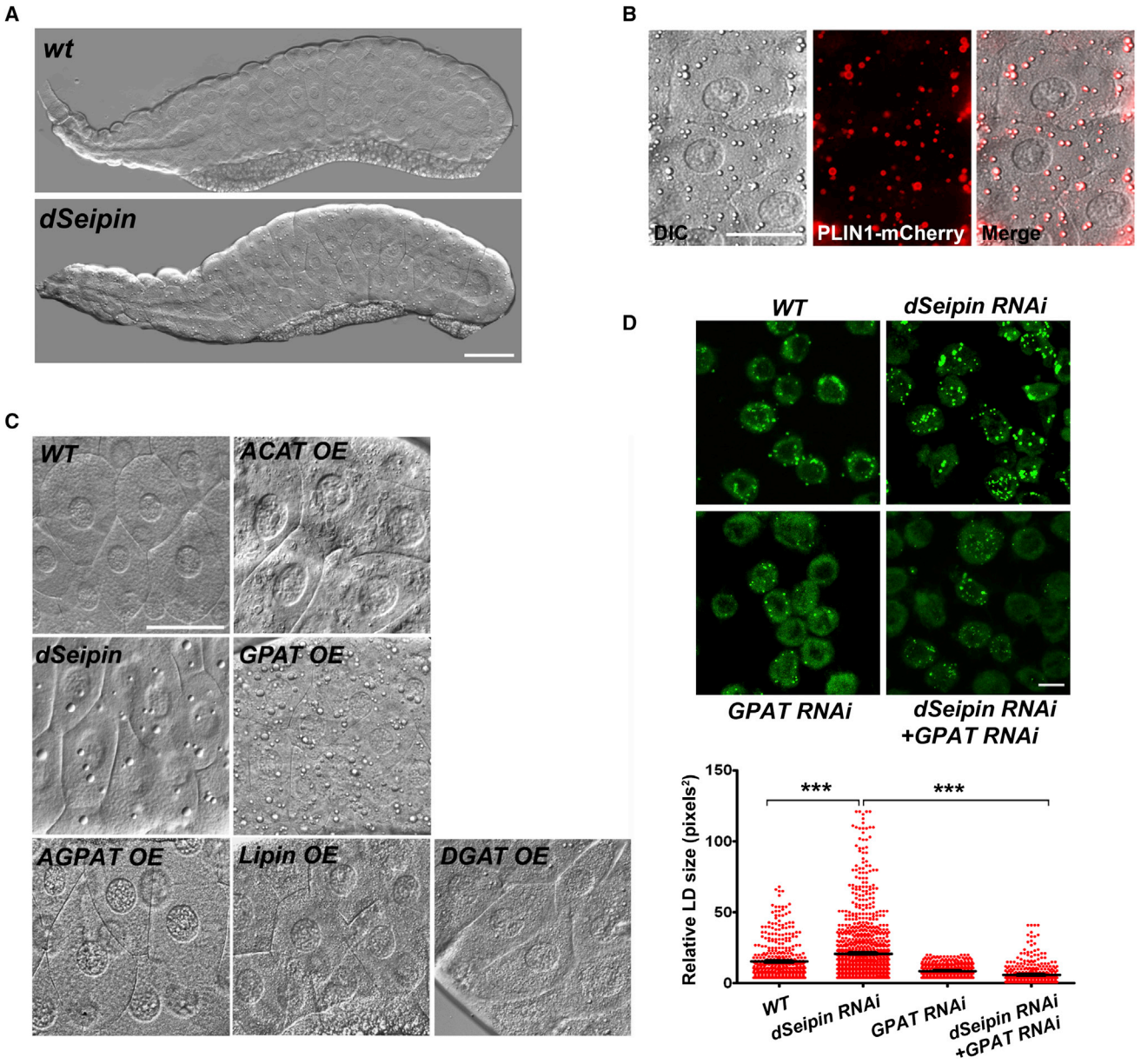

Figure 5. SEIPIN and GPAT Functionally Interact in *Drosophila*

(A–C) GPAT overexpression results in large lipid droplets similar to *dSeipin* mutants in the salivary gland of *Drosophila*. (A) Differential interference contrast (DIC) image of wild-type and *dSeipin* mutant larval salivary gland. Scale bar, 100 μm. (B) The largest lipid droplets in dSeipin mutants can be encircled by lipid droplet surface marker PLIN1-mCherry. The genotype is *dSeipin*; *ppl-Gal4>UAS-PLIN1-mCherry*. Scale bar, 50 μm. (C) DIC images of third-instar larval salivary gland of different genotypes. *GPAT* (*Drosophila* gene *CG5508*), *AGPAT* (*CG17608*), *Lipin* (*CG8709*), *DGAT* (*CG31991*), and *ACAT* (*CG8112*) were each overexpressed using the *ppl-Gal4* promoter. Scale bar, 50 μm.

(D) RNAi-mediated knockdown of SEIPIN in *Drosophil*a S2 cells increases LD size, which can be suppressed by simultaneously knocking down GPAT. Representative confocal images of RNAi-treated and BODIPY-stained cells are shown. Scale bar, 10 μm. Statistical testing utilized one-way ANOVA with a post-Tukey's multiple comparison test. Error bars represent ± SEM. ***$p < 0.001$.

Increased GPAT3 Activity Impairs Adipogenesis in SEIPIN-Deficient Cells

If SEIPIN deficiency increases GPAT activity sufficiently to block adipogenesis, then reducing GPAT in SEIPIN-deficient cells should be able to restore adipogenesis. As predicted, in *Seipin*-deficient 3T3L1 preadipocytes, knocking down *Gpat3*, but not *Gpat4*, significantly enhanced adipocyte differentiation (Figures 6C, 6D, S6D, and S7A–S7E). Finally, to determine whether the increased GPAT activity is sufficient to block adipocyte differentiation, we overexpressed *Gpat3* or *Gpat4* in 3T3L1 preadipocytes. Overexpression of *Gpat3* blocked adipogenesis (Figures S7F–S7H), whereas overexpressing *Gpat4* had only a

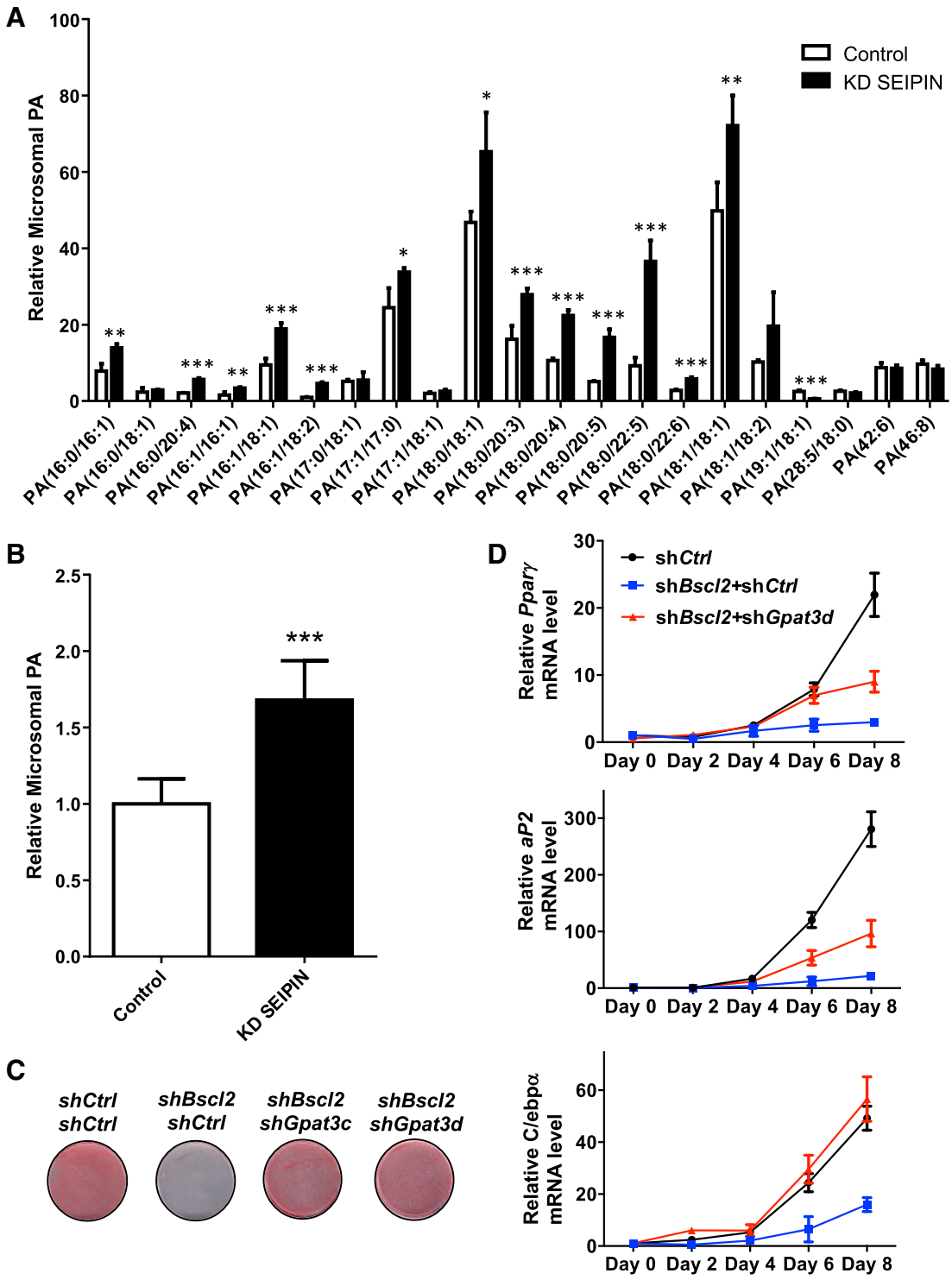

Figure 6. Increased GPAT3 Activity Impairs Adipogenesis in SEIPIN-Deficient Preadipocytes

(A and B) Lipidomic analysis of microsomal PA in control and *shBSCL2* 3T3L1 preadipocytes. Phospholipids were extracted from cells, subjected to HPLC MS/MS, and analyzed using Lipid Search software. n = 4. *p < 0.05; **p < 0.01; ***p < 0.001.

(C) Oil red O stains of differentiated/undifferentiated 3T3-L1 cells stably transfected with the indicated lentiviral knockdown vectors.

(D) *Pparγ*, *aP2* and *C/ebpα* mRNA levels were measured by qRT-PCR in 3T3-L1 cells transduced with the indicated lentiviral knockdown vectors at the indicated time points after induction of differentiation. All experiments were performed in triplicate. See also Figures S6 and S7.

moderate inhibitory effect on adipogenesis (data not shown). Importantly, the simultaneous overexpression of *Seipin* and *Gpat3* restored normal differentiation (Figure S7F–S7H). Taken together, these findings strongly support the interpretation that increased GPAT activity underlies the block in adipogenesis in *Seipin*-deficient cells.

GPAT Inhibitor Partially Rescues the Differentiation of Seipin$^{-/-}$ Preadipocytes

Our results above strongly suggest that pharmacological inhibition of GPAT activity may also restore the differentiation of SEIPIN-deficient cells. Thus, we isolated primary preadipocytes from control and *Seipin*-deficient mice and differentiated them in the presence or absence of a GPAT inhibitor (formula: C21H26ClNO4S) (Outlaw et al., 2014; Wydysh et al., 2009). The inhibition was competitive for NEM-sensitive (microsomal) and NEM-resistant (mitochondrial) GPAT activities (Figure 7A). Inhibition of GPAT at 40 μM increased the number of cells positively stained with Oil red O, as well as the expression of adipogenesis marker genes in *Seipin*$^{-/-}$ cells (Figures 7B and 7C).

DISCUSSION

SEIPIN's role in mammalian lipid storage is unique, because it regulates both adipocyte differentiation and the expansion of cellular LDs (Fei et al., 2011a). However, as an integral membrane protein of the ER without known functional domains, SEIPIN's mechanism of action has been difficult to understand. Here, we demonstrate that SEIPIN and its yeast ortholog, Fld1, can interact specifically with the ER-located GPAT isoforms and that this evolutionarily conserved interaction diminishes the specific activity of both yeast and mammalian GPAT isoforms and alters their substrate affinities. Our data provide strong evidence that when SEIPIN is absent, enhanced microsomal GPAT activity results in defective adipogenesis and altered LD morphology.

The acylation of glycerol-3-P, catalyzed by GPAT, is the initial and rate-limiting step in the synthesis of triacylglycerol and the glycerophospholipids. The mitochondrial isoform GPAT1 contributes between 20% and 50% of the total GPAT activity in liver but only ~10% of total GPAT activity in other tissue types (Coleman and Mashek, 2011). A second mitochondrial GPAT isoform, GPAT2, is expressed primarily in testes. The microsomal GPAT isoforms, GPAT3 and GPAT4, have an 80% amino acid identity and, like the two Gat isoforms in yeast, are integral membrane proteins of the ER (Marr et al., 2012) but may move to the surface of LDs during LD expansion (Wilfling et al., 2013). Similarly, yeast Gat1 may be present on LDs during the stationary phase of yeast growth (Marr et al., 2012). Insulin increases the activities of mammalian GPAT3 and GPAT4 by phosphorylation at Ser and Thr residues, although the functional outcome of these modifications is unclear (Shan et al., 2010). Overall, the regulation of the ER GPATs remains largely unexplored, and no GPAT-interacting proteins have previously been identified.

Through a non-biased screen in yeast, we identified the yeast GPAT, Gat1, as a potential interacting partner of the yeast SEIPIN ortholog, Fld1. Multiple lines of evidence support a specific physical association between orthologs of SEIPIN and ER GPATs. Yeast and mammalian SEIPIN were co-immunoprecipitated with their respective yeast and mammalian GPAT orthologs, and both biotinylation and proximity ligation assays confirmed the close proximity of SEIPIN and GPAT3/4. Interestingly, compared to wild-type SEIPIN, the disease-causing missense mutant T78A had a weakened association with GPAT3/4. These data strongly support a specific physical association between SEIPIN and GPAT3/4. However, because both SEIPIN and the ER GPATs are integral membrane proteins that have resisted purification, we are unable to determine their stoichiometry in vitro or whether their interaction is direct. Because SEIPIN forms oligomers (Sim et al., 2013; Binns et al., 2010; Fei et al., 2011b), it is possible that a single GPAT3/4 molecule may interact with a SEIPIN oligomer. Moreover, whether SEIPIN missense mutants such as T78A cause lipodystrophies through reduced interaction with GPAT remains inconclusive, and future studies will focus on this aspect.

The specific link between orthologs of SEIPIN and the ER GPAT isoforms was strongly and consistently supported by functional assays. SEIPIN deficiency is associated with two striking phenotypes: (1) a near complete block in adipogenesis and (2) the enlargement of LDs in yeast and in those mammalian cells and tissues in which SEIPIN is normally highly expressed, such as testes and mature adipocytes (Liu et al., 2014; Jiang et al., 2014). SEIPIN's association with the ER GPAT isoforms can explain its roles in adipogenesis and LD expansion. As illustrated in Figure S8, our data support the hypothesis that when SEIPIN interacts with the ER GPATs, their enzymatic activity is reduced and the production of PA is diminished. Thus, the normal interaction of SEIPIN and the ER GPAT isoforms results in two major consequences: (1) because PA inhibits PPARγ, low GPAT activity during the first few hours of adipocyte differentiation permits PPARγ to be fully active, so that normal adipogenesis can proceed; and (2) in mature adipocytes, yeast, and other cells, SEIPIN-regulated ER GPAT activity controls the size of LDs, possibly by limiting the amount of fusogenic PA (Figure S7). Conversely, in the absence of SEIPIN, ER GPAT-specific activity is enhanced and PA production increases. The high PA concentration may inhibit PPARγ activity or other signaling pathways in preadipocytes, thereby blocking adipogenesis (Stapleton et al., 2011; Zhang et al., 2012b; Nadra et al., 2012). In other cells, the absence of SEIPIN also results in high GPAT activity and increased local production of PA at the ER, resulting in aberrant LD budding and growth and the formation of supersized LDs (Fei et al., 2011c). Several critical experiments support this interpretation, including the altered GPAT kinetics when SEIPIN is absent, the near-normal adipocyte differentiation that occurs when both SEIPIN and GPAT3 are absent, the formation of supersized LDs when the ER GPATs are overexpressed, and the reduction in LD size when SEIPIN and GPAT are co-expressed.

SEIPIN has been reported to interact with two other glycerolipid synthetic enzymes, AGPAT2 and LIPIN1 (Talukder et al., 2015; Sim et al., 2012). However, there is a fundamental difference between those studies and ours. SEIPIN was proposed to facilitate AGPAT2 and LIPIN1 function, whereas our data suggest that SEIPIN inhibits GPATs. Moreover, although the interaction of SEIPIN with AGPAT2 and LIPIN1 is relevant for the metabolism of PA, GPAT is recognized as the rate-limiting enzyme in the pathway. Importantly, the notion that SEIPIN anchors and

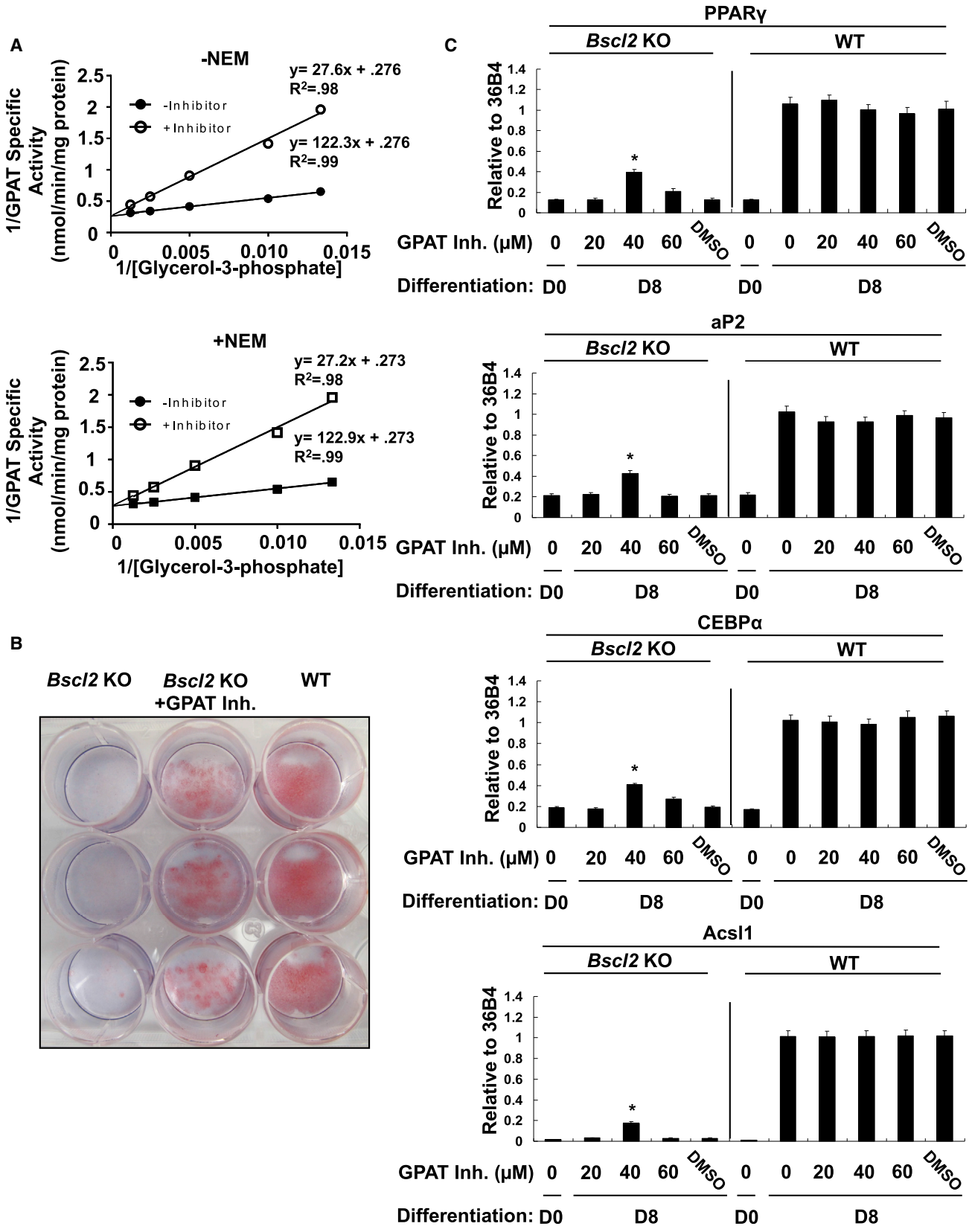

(legend on next page)

facilitates LIPIN function overlooks existing physiological evidence (Talukder et al., 2015). For example, depleting lipin-1 in mouse adipocytes reduces the size of LDs, whereas depleting Seipin in mouse adipocytes increases LD size (Nadra et al., 2012; Liu et al., 2014). Furthermore, our co-immunoprecipitation study in yeast could not detect a SEIPIN-LIPIN1 interaction (data not shown), and the yeast AGPAT2 homolog, Slc4, did not co-precipitate well with Fld1. Importantly, when overexpressed in the salivary gland of *Drosophila* under the same promoter, GPAT is the only enzyme that gave rise to supersized LDs.

In *Drosophila*, SEIPIN has been reported to interact with sarco/endoplasmic reticulum calcium ATPase (SERCA), an ER-specific calcium pump (Bi et al., 2014). However, alterations in ER fatty acid and lipid composition are known to inhibit SERCA activity (Fu et al., 2011). Because our results support a primary function of SEIPIN in ER phospholipid metabolism, the disrupted calcium homeostasis observed in SEIPIN-deficient cells may be secondary to an altered ER phospholipid composition. Recent data also suggest that SEIPIN is involved in the vectorial export of TAG from the ER or the stabilization of ER-LD contact sites (Cartwright et al., 2015; Grippa et al., 2015). Our findings described here do not necessarily contradict with those observations; changes in PA concentration/localization of the ER may also impact the vectorial budding of droplets and/or the phospholipid composition of LDs (Wolinski et al., 2015; Han et al., 2015).

Although both GPAT3 and GPAT4 can interact with SEIPIN, they exhibited clear functional differences. Overexpressing either enzyme altered LD morphology at least in Huh7 cells, but only GPAT3 appeared to play a major role in adipogenesis (Shan et al., 2010). Surprisingly, although GPAT3 is highly upregulated in differentiating adipocytes, *Gpat3*$^{-/-}$ mice had relatively modest phenotypic alterations, and decreased weight gain was detected only when *Gpat3*$^{-/-}$ mice were fed a high-fat diet (Cao et al., 2014). GPAT4 is moderately upregulated during adipogenesis, but it is the major microsomal GPAT activity in brown adipose tissue, where its presence is required to limit the oxidation of exogenous fatty acids (Cooper et al., 2015). Murine GPAT4 is known to localize to LDs (Wilfling et al., 2013); however, our data suggest that both ER GPATs can localize to LDs, particularly GPAT3.

Taken as a whole, our data provide strong evidence that SEIPIN interacts with and regulates ER GPATs in mammalian cells, fly, and *S. cerevisiae*. This is the first example of an evolutionarily conserved, physiological regulator of the ER GPATs.

EXPERIMENTAL PROCEDURES

Materials

Strains, primers, plasmids, and antibodies are listed in Tables S3–S7. [^{3}H] Glycerol-3-P was synthesized enzymatically (Chang and Kennedy, 1967).

Isolation of Fld1-Interacting Proteins

Wild-type yeast cells transformed with plasmid pLacYCP-GFP and *fld1Δ* cells transformed with pLacYCP-Fld1-GFP were grown to early stationary phase and then lysed using a bead beater in three different buffers: buffer 1 (25 mM Tris-HCl [pH 8.0], 150 mM NaCl, 0.5% Triton X-100, 0.2 mM EDTA, and 0.2 mM DTT), buffer 2 (20 mM K-HEPES [pH 7.4], 110 mM CH_3CO_2K, 150 mM NaCl, 0.1% Triton X-100, 0.1% Tween 20, and 2 mM $MgCl_2$), and buffer 3 (20 mM K-HEPES [pH 7.4], 110 mM CH_3CO_2K, 150 mM NaCl, 0.1% Triton X-100, 0.1% Tween 20, 46 mM n-octyl-B-D-glucopyranoside, 2 mM $MgCl_2$, and 5% glycerol). Cell lysates were initially incubated with Sepharose CL-4B (GE Healthcare) to pull down proteins interacting with beads, and the supernatants were affinity purified using a GFP-Trap (ChromoTek) (Rothbauer et al., 2008) to pull down proteins interacting with GFP and Fld1-GFP, respectively.

Identification of Fld1-Interacting Candidates

Proteins were eluted from Sepharose and GFP-Trap beads with a low-pH buffer (pH 2) containing 100 mM glycine, neutralized, and separated on 4%–15% Tris-HCl gels (Bio-Rad). After staining with Coomassie brilliant blue R-250 (Sigma), protein bands were digested in-gel with trypsin (Shevchenko et al., 1996), and the sequences of the resultant peptides were determined by liquid chromatography tandem mass spectrometry using LTQ-Orbitrap Velos Pro (Thermo Fisher Scientific) coupled to UltiMate 3000 RSLC (Dionex). A list of candidate interactors was created from proteins identified in at least three Fld1-GFP pull-downs and absent in the controls (Table S1). Proteins were identified by at least two unique unmodified peptides with a score of −20.

Yeast Growth

Yeast cells were grown as described previously (Sherman, 2002).

Mammalian Cell Culture

HeLa, MEF, 3T3-L1, HEK293FT, and Phoenix Eco cells were grown in DMEM, 10% fetal bovine serum (FBS) (Invitrogen), and 100 U/mL penicillin and streptomycin. Cells were transiently transfected with plasmids using Lipofectamine LTX/Plus (Invitrogen). To induce triacylglycerol synthesis and LD formation, cells were incubated for 16 hr with 400 or 800 μM BSA-coupled oleate.

Retro- and Lentivirus Production and Stable Cell Line Generation

pLKO.1-based shRNA lentiviral or pBABE-based retroviral expression constructs (Table S6) were used to generate lentivirus in HEK293T cells or retrovirus in Phoenix Eco cells, respectively. 3T3-L1 cells were incubated for 24 hr with lenti- or retrovirus together with 8 μg/mL polybrene. Stable cells were selected with 4 μg/mL puromycin and/or 800 μg/mL neomycin for 10 days before use or storage in liquid N_2.

Adipocyte culture and differentiation and qRT-PCR were carried out as described previously (Chen et al., 2012; Payne et al., 2008).

Pre-adipocyte Isolation and Differentiation

Animal protocols were approved by the University of North Carolina at Chapel Hill Institutional Animal Care and Use Committee. Mouse preadipocytes were isolated from gonadal adipose tissue. After excising blood vessels, adipose tissue was minced into small pieces, decanted into isolation medium (DMEM supplemented with 25 mM HEPES, 2% BSA, and 2 mg/mL collagenase), and digested for 30 min at 37°C with constant shaking. Suspended cells

Figure 7. GPAT Inhibitor Can Partially Rescue the Differentiation of *Seipin*$^{-/-}$ Preadipocytes

(A) Glycerol-3-phosphate dependence of GPAT was determined by incubating 10–20 μg total particulate in the presence of 82.5 μM 16:0 CoA and varying the concentration of G3P from 10 to 800 μM, in the absence or presence of NEM. All experiments were performed in triplicates. Data are presented as mean ± SEM. See also Figure S6.

(B) The recovery of differentiation (day 8) is shown by Oil red O staining of WT, *Bscl2* KO, and *Bscl2* KO MEF cells treated with 40 μM inhibitor during the first 2 days of differentiation.

(C) Total RNA extracted from wild-type and *Seipin*$^{-/-}$ preadipocytes cultured in the presence or absence of GPAT inhibitor was used to measure the indicated mRNA levels by qPCR. Values represent mean ± SD of three independent experiments performed in triplicate. Statistical analysis was performed using Student's t test. *$p < 0.05$, inhibitor treatment versus DMSO in *Seipin* KO cells.

were then filtered through a 100-μm nylon filter, centrifuged for 5 min at 400 × *g*, and resuspended in DMEM supplemented with 10% newborn calf serum and 100 U/mL penicillin and streptomycin. Differentiation was carried out as described above, and the GPAT inhibitor was present during the first 48 hr of differentiation.

GPAT Activity and Kinetics

The right testis or MEFs and 3T3L1 cells from 10-cm dishes were homogenized in cold medium I (250 mM sucrose, 10 mM Tris [pH 7.4], 1 mM EDTA, 1 mM DTT) using 10 up-and-down strokes with a Teflon-glass motor-driven homogenizer. Total membranes were isolated by centrifuging the homogenate at 100,000 × *g* for 1 hr. GPAT specific activity (initial rates) was assayed for 10 min at room temperature (RT) in a 200 μL reaction mixture containing 75 mM Tris-HCl (pH 7.5), 4 mM $MgCl_2$, 1 mg/mL BSA (essentially fatty-acid-free), 1 mM DTT, 8 mM NaF, 800 μM [^{3}H]glycerol-3-P, and 82.5 μM palmitoyl-CoA. Membrane protein was incubated on ice for 15 min in the presence or absence of 2 mM NEM, which inactivates GPAT isoforms 2, 3, and 4 (Lewin et al., 2004). The reaction was initiated by adding 20 μg (testis), 15 μg (MEFs), or 5 μg (3T3L1) of membrane protein. Reaction products were extracted into 2 mL $CHCl_3$. NEM-resistant activity (GPAT1) was calculated by subtracting NEM-sensitive activity from total activity. To determine the reaction products, 1 mL of the $CHCl_3$ extract was dried under N_2, resuspended in 30 μL $CHCl_3$:CH_3OH (2:1; v/v), and separated by thin-layer chromatography ($CHCl_3$:pyridine:88% formic acid, 50:30:7; v/v). More than 90% of the reaction product was PA, and the remainder was lysophosphatidic acid. [^{3}H]Glycerol-3-P concentrations (40–400 μM) or palmitoyl-CoA concentrations (11.25–150 μM) were varied to analyze enzyme kinetics.

BY4741 and *fld1*Δ cells were collected by centrifuging at 3,000 × *g* for 5 min, rinsed twice in dH_2O, and stored at −80°C until further use. To obtain total membrane fractions, yeast cells were resuspended in 1 mL zymolyase buffer (50 mM potassium phosphate [pH 7.5], 10 mM β-mercaptoethanol) containing 1,000 U zymolyase (Zymo Research). Cell suspensions were shaken at 150 rpm at 30°C for 90 min. The supernatant was then homogenized, and membranes were isolated by centrifugation as described above. To assay GPAT activity in yeast, 20 μg membrane protein was pre-incubated in the presence of 50 μM 16:0 CoA for 1 hr. Reactions were initiated by adding the [^{3}H] glycerol-3-phosphate. To analyze enzyme kinetics in yeast, [^{3}H] glycerol-3-P concentrations (5–400 μM) or palmitoyl-CoA concentrations (12.5–100 μM) were varied.

Co-immunoprecipitation and Western Blotting

Antibodies used are listed in Table S8. Yeast cell lysates were prepared as described previously (Fei et al., 2008). 2 mg protein was used for each co-immunoprecipitation condition. Antibody was immobilized on magnetic Dynabeads (Dynabeads Co-Immunoprecipitation Kit manual). After 30 min of incubation with the cell lysates containing overexpressed protein at RT, or after overnight incubation with the cell lysates containing low levels of recombinant protein at 4°C, beads were washed and eluted at 37°C for 20 min. Proteins were transferred onto polyvinylidene fluoride (PVDF) membranes, followed by immunodetection (Fei et al., 2008).

Transiently or stably transfected mammalian cells (MEFs, mouse 3T3-L1preadipocytes, and HeLa cells) were washed three times with ice-cold PBS and lysed in immunoprecipitation (IP) lysis/wash buffer (as above) containing 1% (w/v) n-dodecyl-β-D-maltopyranoside (DDM; Sigma) by forcing the cells 30 times through a 0.8-mm needle. Immunoprecipitation and western blotting were carried out as described above.

BirA* Pull-Down Assays

The cDNA for BirA* was subcloned from pGEM-SD2-BirA* (a kind gift of John Strouboulis, Erasmus University Medical Center, Rotterdam, the Netherlands). 3T3-L1 preadipocytes were transduced with FLAG-tagged SEIPIN, FLAG-tagged biotin ligase BirA*, or FLAG-tagged BirA*-SEIPIN delivered using retrovirus, and cells were then induced to differentiate to mature adipocytes. On day 8 of differentiation, cells were treated with 50 μM biotin for 24 hr and then lysed. Cell lysates were precleared with empty protein G agarose beads for 4 hr and then incubated with streptavidin-conjugated agarose for 2 hr at room temperature. The beads were collected and washed with buffers as described previously (Roux et al., 2012), incubated with sample buffer containing 1.5 mM biotin, and heated for 1 hr at 65°C before western blot analysis.

Proximity Ligation Assay

HeLa cells transfected with indicated plasmids were fixed with 4% paraformaldehyde (Electron Microscopy Sciences) for 15 min and permeabilized with 0.2% Triton X-100 (Sigma-Aldrich) for 10 min at room temperature. Cells were then blocked with 3% BSA in PBS for 1 hr and incubated with appropriate combinations of mouse anti-FLAG (1:100; Clontech Laboratories) and rabbit anti-HA (1:3,000; CST) antibodies diluted in blocking solution for 1 hr at room temperature. This was followed by proximity ligation assay using the Duolink detection reagent kit (Olink Bioscience) according to the manufacturer's protocol. Fluorescence images were acquired using an Olympus Fluoview FV1200 confocal microscope with a 60×/1.35 UPlanSApo objective. Images were prepared and analyzed with Fiji software (http://fiji.sc). For each experiment, signals from at least 50 cells were quantified. All data were analyzed using GraphPad PRISM software.

Fluorescence Microscopy

Yeast cells were stained with 20 μg/mL Nile red (Sigma-Aldrich). For mammalian lipid droplets, BODIPY 493/503 (Invitrogen) was used. Imaging was performed using a Leica SP5 confocal microscope and a Leica HCX 63× 1.4 numerical aperture objective.

Lipidomic Analysis of Microsomal PA

Phospholipids were extracted from microsomes isolated from yeast or mammalian cells, subjected to high performance liquid chromatography (HPLC) tandem mass spectrometry (MS/MS) and analyzed using Lipid Search software as described (Qi et al., 2016; Fei et al., 2011c).

Drosophila experiments are as described previously (Tian et al., 2011). *ppl-Gal4* was used to drive the overexpression of genes indicated.

Statistics

Experiments were performed in triplicate. The results are presented as mean ± SD. Two-tailed Student's t test was used for comparison.

SUPPLEMENTAL INFORMATION

Supplemental Information includes eight figures and seven tables and can be found with this article online at http://dx.doi.org/10.1016/j.celrep.2016.10.037.

AUTHOR CONTRIBUTIONS

M.P., D.E.C., Y.Q., G.L., X.H., R.A.C., and H.Y. designed the research, wrote the manuscript, and contributed to the writing of the final submitted version of the manuscript. M.P., D.E.C., I.L., Z.W., Y.T., Z.L., C.F., R.G.P., M.L., H.Y.M., T.K., D.K., P.S., X.D., Y.Q., and T.E.H. performed experiments and analyzed data. W.C. provided critical reagents. R.A.C. and H.Y. are the guarantors of this work, had full access to all the data in the study, and take responsibility for the integrity of the data and the accuracy of the data analysis.

ACKNOWLEDGMENTS

Mass spectrometric analysis was performed at the Bioanalytical Mass Spectrometry Facility, University of New South Wales and supported in part by infrastructure funding from the New South Wales Government. H.Y. was supported by grants 1057852 and 1078117 from the National Health and Medical Research Council, Australia, and by grants DP130100457 and DP120101543 from the Australian Research Council. H.Y. is a Senior Research Fellow of the NHMRC. R.A.C. was supported by NIH grant DK56598.

Received: March 9, 2016
Revised: September 3, 2016
Accepted: October 10, 2016
Published: November 1, 2016

REFERENCES

Agarwal, A.K., and Garg, A. (2006). Genetic basis of lipodystrophies and management of metabolic complications. Annu. Rev. Med. *57*, 297–311.

Bi, J., Wang, W., Liu, Z., Huang, X., Jiang, Q., Liu, G., Wang, Y., and Huang, X. (2014). Seipin promotes adipose tissue fat storage through the ER Ca^{2+}-ATPase SERCA. Cell Metab. *19*, 861–871.

Binns, D., Lee, S., Hilton, C.L., Jiang, Q.X., and Goodman, J.M. (2010). Seipin is a discrete homooligomer. Biochemistry *49*, 10747–10755.

Cao, G., Konrad, R.J., Li, S.D., and Hammond, C. (2012). Glycerolipid acyltransferases in triglyceride metabolism and energy homeostasis-potential as drug targets. Endocr. Metab. Immune Disord. Drug Targets *12*, 197–206.

Cao, J., Perez, S., Goodwin, B., Lin, Q., Peng, H., Qadri, A., Zhou, Y., Clark, R.W., Perreault, M., Tobin, J.F., and Gimeno, R.E. (2014). Mice deleted for GPAT3 have reduced GPAT activity in white adipose tissue and altered energy and cholesterol homeostasis in diet-induced obesity. Am. J. Physiol. Endocrinol. Metab. *306*, E1176–E1187.

Cartwright, B.R., and Goodman, J.M. (2012). Seipin: from human disease to molecular mechanism. J. Lipid Res. *53*, 1042–1055.

Cartwright, B.R., Binns, D.D., Hilton, C.L., Han, S., Gao, Q., and Goodman, J.M. (2015). Seipin performs dissectible functions in promoting lipid droplet biogenesis and regulating droplet morphology. Mol. Biol. Cell *26*, 726–739.

Chang, Y.Y., and Kennedy, E.P. (1967). Biosynthesis of phosphatidyl glycerophosphate in Escherichia coli. J. Lipid Res. *8*, 447–455.

Chen, W., Chang, B., Saha, P., Hartig, S.M., Li, L., Reddy, V.T., Yang, Y., Yechoor, V., Mancini, M.A., and Chan, L. (2012). Berardinelli-seip congenital lipodystrophy 2/seipin is a cell-autonomous regulator of lipolysis essential for adipocyte differentiation. Mol. Cell. Biol. *32*, 1099–1111.

Coleman, R.A., and Mashek, D.G. (2011). Mammalian triacylglycerol metabolism: synthesis, lipolysis, and signaling. Chem. Rev. *111*, 6359–6386.

Cooper, D.E., Grevengoed, T.J., Klett, E.L., and Coleman, R.A. (2015). Glycerol-3-phosphate acyltransferase isoform-4 (GPAT4) limits oxidation of exogenous fatty acids in brown adipocytes. J. Biol. Chem. *290*, 15112–15120.

Cui, X., Wang, Y., Tang, Y., Liu, Y., Zhao, L., Deng, J., Xu, G., Peng, X., Ju, S., Liu, G., and Yang, H. (2011). Seipin ablation in mice results in severe generalized lipodystrophy. Hum. Mol. Genet. *20*, 3022–3030.

Fei, W., Shui, G., Gaeta, B., Du, X., Kuerschner, L., Li, P., Brown, A.J., Wenk, M.R., Parton, R.G., and Yang, H. (2008). Fld1p, a functional homologue of human seipin, regulates the size of lipid droplets in yeast. J. Cell Biol. *180*, 473–482.

Fei, W., Du, X., and Yang, H. (2011a). Seipin, adipogenesis and lipid droplets. Trends Endocrinol. Metab. *22*, 204–210.

Fei, W., Li, H., Shui, G., Kapterian, T.S., Bielby, C., Du, X., Brown, A.J., Li, P., Wenk, M.R., Liu, P., and Yang, H. (2011b). Molecular characterization of seipin and its mutants: implications for seipin in triacylglycerol synthesis. J. Lipid Res. *52*, 2136–2147.

Fei, W., Shui, G., Zhang, Y., Krahmer, N., Ferguson, C., Kapterian, T.S., Lin, R.C., Dawes, I.W., Brown, A.J., Li, P., et al. (2011c). A role for phosphatidic acid in the formation of "supersized" lipid droplets. PLoS Genet. *7*, e1002201.

Fu, S., Yang, L., Li, P., Hofmann, O., Dicker, L., Hide, W., Lin, X., Watkins, S.M., Ivanov, A.R., and Hotamisligil, G.S. (2011). Aberrant lipid metabolism disrupts calcium homeostasis causing liver endoplasmic reticulum stress in obesity. Nature *473*, 528–531.

Grippa, A., Buxó, L., Mora, G., Funaya, C., Idrissi, F.Z., Mancuso, F., Gomez, R., Muntanyà, J., Sabidó, E., and Carvalho, P. (2015). The seipin complex Fld1/Ldb16 stabilizes ER-lipid droplet contact sites. J. Cell Biol. *211*, 829–844.

Han, S., Binns, D.D., Chang, Y.F., and Goodman, J.M. (2015). Dissecting seipin function: the localized accumulation of phosphatidic acid at ER/LD junctions in the absence of seipin is suppressed by Sei1p(ΔNterm) only in combination with Ldb16p. BMC Cell Biol. *16*, 29.

Jiang, M., Gao, M., Wu, C., He, H., Guo, X., Zhou, Z., Yang, H., Xiao, X., Liu, G., and Sha, J. (2014). Lack of testicular seipin causes teratozoospermia syndrome in men. Proc. Natl. Acad. Sci. USA *111*, 7054–7059.

Lewin, T.M., Schwerbrock, N.M., Lee, D.P., and Coleman, R.A. (2004). Identification of a new glycerol-3-phosphate acyltransferase isoenzyme, mtGPAT2, in mitochondria. J. Biol. Chem. *279*, 13488–13495.

Liu, L., Jiang, Q., Wang, X., Zhang, Y., Lin, R.C., Lam, S.M., Shui, G., Zhou, L., Li, P., Wang, Y., et al. (2014). Adipose-specific knockout of SEIPIN/BSCL2 results in progressive lipodystrophy. Diabetes *63*, 2320–2331.

Loewen, C.J., Gaspar, M.L., Jesch, S.A., Delon, C., Ktistakis, N.T., Henry, S.A., and Levine, T.P. (2004). Phospholipid metabolism regulated by a transcription factor sensing phosphatidic acid. Science *304*, 1644–1647.

Lundin, C., Nordström, R., Wagner, K., Windpassinger, C., Andersson, H., von Heijne, G., and Nilsson, I. (2006). Membrane topology of the human seipin protein. FEBS Lett. *580*, 2281–2284.

Magré, J., Delépine, M., Khallouf, E., Gedde-Dahl, T., Jr., Van Maldergem, L., Sobel, E., Papp, J., Meier, M., Mégarbané, A., Bachy, A., et al.; BSCL Working Group (2001). Identification of the gene altered in Berardinelli-Seip congenital lipodystrophy on chromosome 11q13. Nat. Genet. *28*, 365–370.

Marr, N., Foglia, J., Terebiznik, M., Athenstaedt, K., and Zaremberg, V. (2012). Controlling lipid fluxes at glycerol-3-phosphate acyltransferase step in yeast: unique contribution of Gat1p to oleic acid-induced lipid particle formation. J. Biol. Chem. *287*, 10251–10264.

Nadra, K., Médard, J.J., Mul, J.D., Han, G.S., Grès, S., Pende, M., Metzger, D., Chambon, P., Cuppen, E., Saulnier-Blache, J.S., et al. (2012). Cell autonomous lipin 1 function is essential for development and maintenance of white and brown adipose tissue. Mol. Cell. Biol. *32*, 4794–4810.

Outlaw, V.K., Wydysh, E.A., Vadlamudi, A., Medghalchi, S.M., and Townsend, C.A. (2014). Design, Synthesis, and Evaluation of 4- and 5-Substituted o-(Octanesulfonamido)benzoic Acids as Inhibitors of Glycerol-3-Phosphate Acyltransferase. MedChemComm *5*, 826–830.

Payne, V.A., Grimsey, N., Tuthill, A., Virtue, S., Gray, S.L., Dalla Nora, E., Semple, R.K., O'Rahilly, S., and Rochford, J.J. (2008). The human lipodystrophy gene BSCL2/seipin may be essential for normal adipocyte differentiation. Diabetes *57*, 2055–2060.

Polokoff, M.A., and Bell, R.M. (1978). Limited palmitoyl-CoA penetration into microsomal vesicles as evidenced by a highly latent ethanol acyltransferase activity. J. Biol. Chem. *253*, 7173–7178.

Prieur, X., Dollet, L., Takahashi, M., Nemani, M., Pillot, B., Le May, C., Mounier, C., Takigawa-Imamura, H., Zelenika, D., Matsuda, F., et al. (2013). Thiazolidinediones partially reverse the metabolic disturbances observed in Bscl2/seipin-deficient mice. Diabetologia *56*, 1813–1825.

Qi, Y., Kapterian, T.S., Du, X., Ma, Q., Fei, W., Zhang, Y., Huang, X., Dawes, I.W., and Yang, H. (2016). CDP-diacylglycerol synthases regulate the growth of lipid droplets and adipocyte development. J. Lipid Res. *57*, 767–780.

Rothbauer, U., Zolghadr, K., Muyldermans, S., Schepers, A., Cardoso, M.C., and Leonhardt, H. (2008). A versatile nanotrap for biochemical and functional studies with fluorescent fusion proteins. Mol. Cell. Proteomics *7*, 282–289.

Roux, K.J., Kim, D.I., Raida, M., and Burke, B. (2012). A promiscuous biotin ligase fusion protein identifies proximal and interacting proteins in mammalian cells. J. Cell Biol. *196*, 801–810.

Shan, D., Li, J.L., Wu, L., Li, D., Hurov, J., Tobin, J.F., Gimeno, R.E., and Cao, J. (2010). GPAT3 and GPAT4 are regulated by insulin-stimulated phosphorylation and play distinct roles in adipogenesis. J. Lipid Res. *51*, 1971–1981.

Sherman, F. (2002). Getting started with yeast. Methods Enzymol. *350*, 3–41.

Shevchenko, A., Wilm, M., Vorm, O., and Mann, M. (1996). Mass spectrometric sequencing of proteins silver-stained polyacrylamide gels. Anal. Chem. *68*, 850–858.

Sim, M.F., Dennis, R.J., Aubry, E.M., Ramanathan, N., Sembongi, H., Saudek, V., Ito, D., O'Rahilly, S., Siniossoglou, S., and Rochford, J.J. (2012). The human lipodystrophy protein seipin is an ER membrane adaptor for the adipogenic PA phosphatase lipin 1. Mol. Metab. *2*, 38–46.

Sim, M.F., Talukder, M.M., Dennis, R.J., O'Rahilly, S., Edwardson, J.M., and Rochford, J.J. (2013). Analysis of naturally occurring mutations in the human lipodystrophy protein seipin reveals multiple potential pathogenic mechanisms. Diabetologia *56*, 2498–2506.

Söderberg, O., Gullberg, M., Jarvius, M., Ridderstråle, K., Leuchowius, K.J., Jarvius, J., Wester, K., Hydbring, P., Bahram, F., Larsson, L.G., and Landegren, U. (2006). Direct observation of individual endogenous protein complexes in situ by proximity ligation. Nat. Methods *3*, 995–1000.

Stapleton, C.M., Mashek, D.G., Wang, S., Nagle, C.A., Cline, G.W., Thuillier, P., Leesnitzer, L.M., Li, L.O., Stimmel, J.B., Shulman, G.I., and Coleman, R.A. (2011). Lysophosphatidic acid activates peroxisome proliferator activated receptor-γ in CHO cells that over-express glycerol 3-phosphate acyltransferase-1. PLoS ONE *6*, e18932.

Szymanski, K.M., Binns, D., Bartz, R., Grishin, N.V., Li, W.P., Agarwal, A.K., Garg, A., Anderson, R.G., and Goodman, J.M. (2007). The lipodystrophy protein seipin is found at endoplasmic reticulum lipid droplet junctions and is important for droplet morphology. Proc. Natl. Acad. Sci. USA *104*, 20890–20895.

Talukder, M.M., Sim, M.F., O'Rahilly, S., Edwardson, J.M., and Rochford, J.J. (2015). Seipin oligomers can interact directly with AGPAT2 and lipin 1, physically scaffolding critical regulators of adipogenesis. Mol. Metab. *4*, 199–209.

Tian, Y., Bi, J., Shui, G., Liu, Z., Xiang, Y., Liu, Y., Wenk, M.R., Yang, H., and Huang, X. (2011). Tissue-autonomous function of Drosophila seipin in preventing ectopic lipid droplet formation. PLoS Genet. *7*, e1001364.

Wang, C.W., Miao, Y.H., and Chang, Y.S. (2014). Control of lipid droplet size in budding yeast requires the collaboration between Fld1 and Ldb16. J. Cell Sci. *127*, 1214–1228.

Wendel, A.A., Lewin, T.M., and Coleman, R.A. (2009). Glycerol-3-phosphate acyltransferases: rate limiting enzymes of triacylglycerol biosynthesis. Biochim. Biophys. Acta *1791*, 501–506.

Wilfling, F., Wang, H., Haas, J.T., Krahmer, N., Gould, T.J., Uchida, A., Cheng, J.X., Graham, M., Christiano, R., Fröhlich, F., et al. (2013). Triacylglycerol synthesis enzymes mediate lipid droplet growth by relocalizing from the ER to lipid droplets. Dev. Cell *24*, 384–399.

Wolinski, H., Hofbauer, H.F., Hellauer, K., Cristobal-Sarramian, A., Kolb, D., Radulovic, M., Knittelfelder, O.L., Rechberger, G.N., and Kohlwein, S.D. (2015). Seipin is involved in the regulation of phosphatidic acid metabolism at a subdomain of the nuclear envelope in yeast. Biochim. Biophys. Acta *1851*, 1450–1464.

Wydysh, E.A., Medghalchi, S.M., Vadlamudi, A., and Townsend, C.A. (2009). Design and synthesis of small molecule glycerol 3-phosphate acyltransferase inhibitors. J. Med. Chem. *52*, 3317–3327.

Zhang, C., Wendel, A.A., Keogh, M.R., Harris, T.E., Chen, J., and Coleman, R.A. (2012a). Glycerolipid signals alter mTOR complex 2 (mTORC2) to diminish insulin signaling. Proc. Natl. Acad. Sci. USA *109*, 1667–1672.

Zhang, P., Takeuchi, K., Csaki, L.S., and Reue, K. (2012b). Lipin-1 phosphatidic phosphatase activity modulates phosphatidate levels to promote peroxisome proliferator-activated receptor γ (PPARγ) gene expression during adipogenesis. J. Biol. Chem. *287*, 3485–3494.

Zhang, C., Cooper, D.E., Grevengoed, T.J., Li, L.O., Klett, E.L., Eaton, J.M., Harris, T.E., and Coleman, R.A. (2014). Glycerol-3-phosphate acyltransferase-4-deficient mice are protected from diet-induced insulin resistance by the enhanced association of mTOR and rictor. Am. J. Physiol. Endocrinol. Metab. *307*, E305–E315.